# First-principles and semiempirical Hartree-Fock calculations for $F$ centers in $KNbO_3$ and Li impurities in $KTaO_3$

R. I. Eglitis[a,b], E. A. Kotomin[b,c], A. V. Postnikov[a], N. E. Christensen[c], and G. Borstel[a]

[a] *Universität Osnabrück – Fachbereich Physik, D-49069 Osnabrück, Germany*
[b] *Institute of Solid State Physics, University of Latvia, 8 Kengaraga, Riga LV-1063, Latvia*
[c] *Institute of Physics and Astronomy, University of Aarhus Aarhus C, DK-8000, Denmark*

(Received 4 February 1998)

**Abstract.** The linear muffin-tin-orbital method based on the density-functional theory and the semi-empirical method of the Intermediate Neglect of the Differential Overlap based on the Hartree–Fock formalism are used for the supercell study of the $F$ centers in cubic and orthorhombic ferroelectric $KNbO_3$ crystals. Two electrons are found to be considerably delocalized even in the ground state of the defect. The absorption energies were calculated by means of the INDO method using the $\Delta$SCF scheme after a relaxation of atoms surrounding the $F$ center.

As an example of another type of point defect in perovskite, an isolated Li impurity in $KTaO_3$ as well as interacting Li pairs are considered in the supercell approach, using the supercells of up to 270 atoms. The off-center Li displacement, reorientational energy barriers and the lattice relaxation around impurities are calculated. The results are compared with those obtained earlier within the shell model, revealing the relaxation pattern somehow different from the shell model estimations.

## INTRODUCTION

It is well understood now that point defects play an important role in the electro-optic and non-linear optical applications of $KNbO_3$ and related materials [1]. In particular, the light frequency doubling in $KNbO_3$ is seriously affected by unidentified defects responsible for the induced IR absorption [2]. The photorefractive effect, important in particular for holographic storage, is also known to depend on the presence of impurities and defects.

One of the most common defects in oxide crystals is the so-called $F$ center, an O vacancy $V_O$ which traps two electrons [3]. In electron-irradiated $KNbO_3$, a broad absorption band is observed around 2.7 eV at room temperature and tentatively ascribed to $F$ centers [4,5]. The motivation behind the present study of this defect by

means of theory is twofold. First, due to the lowering of the local point symmetry at the O site in ferroelectric phases of $KNbO_3$ (for instance, in the orthorhombic phase which is the room-temperature one), the degeneracy of the $2p$-type excited state may be lifted, resulting in several splitted absorption bands. Second, there were claims in the literature in favor of the symmetry breaking between two Nb atoms neighboring the O vacancy, resulting in an asymmetric electron density distribution [6]. In order to clarify these questions and to check the assignment of the 2.7 eV absorption band, we study in the present paper the $F$ center in $KNbO_3$ using the supercell model and two different theoretical techniques: the full-potential linear muffin-tin orbital (FP-LMTO) and the semiempirical Intermediate Neglect of the Differential Overlap (INDO) methods. In the present contribution we essentially summarize the results presented recently in more detail in Ref. [7].

The same techniques, also in the supercell approach, have been applied to the study of another point defect, inducing lattice relaxation in a incipient ferroelectric crystal: Li substituting K in $KTaO_3$. As is experimentally known [8], such substitutional impurity gets spontaneously displaced along one of six possible [100]-type directions. The magnitude of this displacement and (in some cases) the lattice relaxation related to it have been estimated by empirical models [9,10], the shell model [11,12], first-principles FP-LMTO calculations [13] and recently by the INDO method [14]. As an extension of the latter study, we discuss in the present contribution also the effects of interaction between Li impurities by the same method. The INDO method has an advantage of being relatively compact in what regards the necessary computer resources. This allows in the study of impurity systems to treat relatively large supercells which remain well beyond the range of *ab initio* total-energy methods. At the same time, once the essential parameters of the INDO method are known for the system in question, the description of excitation energies and/or total-energy trends with the INDO method is much better than within any model schemes.

The INDO method is described in detail in Ref. [15]. We used its practical implementation in the computer code CLUSTERD. The technical details related to the application of method (e.g. parametrisation) for $KNbO_3$ can be found in Ref. [16], for Li-doped $KTaO_3$ – in Ref. [14]. As a benchmark for the INDO parametrisation in the previous study [16,14], as well as for independent investigation of the $F$-center in Ref. [7] (the essential results of which are discussed below), we used the FP-LMTO method in the implementation by M. Methfessel [17].

## TECHNICAL DETAILS OF CALCULATION AND RESULTS FOR F-CENTERS

In both LMTO and INDO calculations of the oxygen vacancy in $KNbO_3$, we used $2\times2\times2$ supercells, including 39 atoms, for the geometry of ideal cubic perovskite lattice. A more detailed study of $F$-center system within the local density approximation, using e.g. the atomic sphere approximation along with the FP-LMTO, the

electronic structure of the defect system and the aspects of correcting the band gap are discussed in Ref. [7] and skipped here. Summarizing, the band gap estimated from the ground-state band structure in the local density approximation (LDA), as is not justified but commonly used, is known to be underestimated in dielectrics. This does not present a problem for the total-energy studies (even structure optimizations) in pure oxides, but in case of the $F$-center the impurity band formed in the band gap exhibits too strong dispersion (due to limited supercell size) and overlaps with the states in the conduction band, resulting in a metallic behavior of the impurity system. In the INDO calculation which is essentially a Hartree-Fock scheme and hence tends to overestimate the band gap, no such problem arises. On the other hand, we would like to keep the LDA results as a useful reference point for the electronic structure and as a reliable benchmark of the total energy-based structure optimization. It can be achieved either by an artificial operator shifting the Nb4$d$ states in the conduction band upwards (that is useful for the analysis of the electronic structure but makes the total energy results unreliable), or by performing the total energy calculation with only one **k**-point in the Brillouin zone, in order to suppress the dispersion of the defect states. In the latter case, the calculation setup becomes somehow resembling that of INDO, where also only the $\Gamma$ point is traditionally used for the **k**-space sampling, in the spirit of the "large unit cell" (LUC) scheme [18]. Since the structure optimization normally needs good convergency in the number of **k**-points, the total-energy result of such LDA calculation should be considered as an approximate one, giving rather an error bar when taken together with that of INDO. According to the LDA calculation, the relaxation of two Nb atoms neighboring to the $F$ center is outwards by 4.8% of the lattice constant, resulting in the energy lowering by 1.2 eV. From the INDO calculation, both values are somehow larger but in qualitative agreement with the LDA results: outward relaxation of two Nb neighbors by 6.5% and the energy gain of $\sim$3.7 eV.

In addition to analyzing this most important aspect of relaxation, we optimized in the INDO calculation the positions of more distant neighbors (14 atoms in total) to the O vacancy as well. The 0.9% outward displacement of K atoms and the 1.9% inward displacement of O atoms gives the total relaxation energy of $\sim$4.7 eV, mostly due to the contributions from the Nb and O displacements.

The analysis of the effective charges of atoms surrounding the $F$ center shows that of the two electrons associated with the removed O atom, only $\approx -0.6|e|$ is localized at the vacancy, and about a similar extra charge is localized on the two nearest Nb atoms. The $F$ center produces a local energy level $\approx 0.6$ eV above the top of the valence band. Its molecular orbital contains primarily contribution from the atomic orbitals of the two nearest Nb atoms.

The structure optimization based on the INDO calculation has also been done for a low-symmetry geometry corresponding to a room-temperature (ferroelectric) orthorhombic phase of $KNbO_3$. This phase is stable in a broad temperature range (263 to 498 K) and hence subject to most studies and practical applications. The structure parameters in pure $KNbO_3$ have been optimized with the INDO method

**TABLE 1.** Calculated absorption energy for the $F$ center ($E_{abs}$) and the energy of the nearest-neighbors Nb relaxation ($E_{rel}$) in cubic and orthorhombic phases of $KNbO_3$.

| Symmetry, phase | $E_{abs}$ (eV) | | | $E_{rel}$ (eV) |
|---|---|---|---|---|
| $C_{4v}$, cubic | 2.73 | 2.97 | – | 3.7 |
| $C_s$, orthorhombic | 2.56 | 3.03 | 3.10 | 3.6 |
| $C_{2v}$, orthorhombic | 2.72 | 3.04 | 3.11 | 3.6 |

in Ref. [16] and are in quite good agreement with the experimental measurements. In the orthorhombic phase, there are two inequivalent positions of oxygen and hence the possibility to form two different kinds of $F$-center, possibly with different optical properties. The displacements of Nb atoms nearest to $V_{\rm O}$ were calculated for these both types of defects and found to be very close to those found for the cubic phase. The relevant relaxation energies (3.6 eV) and also nearly the same as for the Nb relaxation found in the cubic phase.

Because of different local symmetry at the O site (either $C_{2v}$ or $C_s$, in contrast to $C_{4h}$ in the cubic phase), the energetics of the impurity levels changes. In the cubic phase, the $V_{\rm O}$ excited state splits into two levels, one of which remains two-fold degenerate. Our $\Delta$SCF calculations predict the two relevant vacant bands, the absorption energies of which are given in Table 1. In the orthorhombic phase, the degeneracy of the impurity level is completely lifted (Table 1). The relaxation energies (associated with the Displacement of Nb neighbors only) are also listed in Table 1 for comparison.

## OFF-CENTER DISPLACEMENT OF Li IN $KTaO_3$ AND RELATED LATTICE RELAXATION

The off-center displacement of substitutional Li in $KTaO_3$ is known to induce a considerable long-range polarization of crystal. Therefore the supercell size needs to be larger than for the study of $F$ centers. The size of the polarized region associated with the [100]-displaced Li ion was estimated in the shell model calculation by Stachiotti and Migoni [11] to be about 5 lattice constants along the direction of displacement, with ∼99% of the 'effective dipole' polarization being confined to nearest Ta–O chains, that go parallel to the displacement. As is discussed below, the magnitudes of the atomic displacements and polarization in our present calculation is considerably smaller than those found in Ref. [11], and the relaxed neighbors to the Li impurity are well within the $3\times3\times3$ supercell. In order to be on safer side, we performed as well the calculations for a supercell doubled in the direction of Li displacement, i.e., $6\times3\times3$, with a single [100]-displaced Li atom. The equilibrium displacement in this case is 0.62 Å, exactly as for the $3\times3\times3$ supercell, with the energy lowering 57.2 meV. The difference from the result for a $3\times3\times3$ supercell (62.0 meV) roughly represents the uncertainty related to the supercell size in our

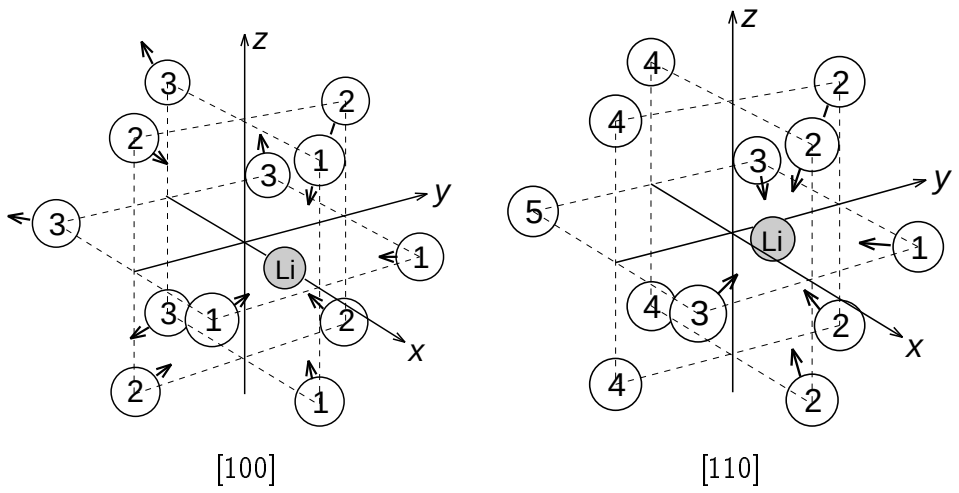


**FIGURE 1.** [100] and [110] Li off-center displacements and the relaxation pattern of neighboring oxygen atoms.

calculations.

The parametrisation of the INDO method for the $KTaO_3$:Li system has been done in Ref. [14] based on the comparison with the results of earlier FP-LMTO calculations [13] in what regards the magnitude of the Li off-center displacement (0.61 Å [13]) as well as the energy gain due to the Li displacement. The total energy as function of [100] and [110] Li off-center displacements as calculated by INDO is shown in Fig. 2. Our equilibrium [100] off-center displacement of 1.44 Å from the shell model by Stachiotti and Migoni within the shell model [11]. On the other hand, our value is in good agreement with a more recent, and apparently more elaborately parameterized, shell model calculation by Exner *et al.* (0.64 Å, Ref. [12]).

**TABLE 2.** Relaxed atomic positions for the Li displacement as calculated by INDO.

| Atom | Lattice coordinates | | | Displacement |
|---|---|---|---|---|
| | | | Li [100] displacement | |
| Li | $\Delta_x$ | 0 | 0 | $\Delta_x = 0.1550$ |
| 4×O(1) | $\frac{1}{2}+\Delta_x$ | $\frac{1}{2}+\Delta_y$ | 0 | $\Delta_x = -0.0045$; $\Delta_y = -0.0105$ |
| 4×O(2) | $\Delta_x$ | $\frac{1}{2}+\Delta_y$ | $\frac{1}{2}+\Delta_y$ | $\Delta_x = 0.0070$; $\Delta_y = -0.0026$ |
| 4×O(3) | $-\frac{1}{2}+\Delta_x$ | $\frac{1}{2}+\Delta_y$ | 0 | $\Delta_x = -0.0020$; $\Delta_y = 0.0020$ |
| | | | Li [110] displacement | |
| Li | $\Delta_x$ | $\Delta_x$ | 0 | $\Delta_x = 0.0760$ |
| 1×O(1) | $\frac{1}{2}+\Delta_x$ | $\frac{1}{2}+\Delta_x$ | 0 | $\Delta_x = -0.0090$ |
| 4×O(2) | $\frac{1}{2}+\Delta_x$ | $\Delta_y$ | $\frac{1}{2}+\Delta_z$ | $\Delta_x = -0.0060$; $\Delta_y = 0.0030$; $\Delta_z = -0.0080$ |
| 2×O(3) | $\frac{1}{2}+\Delta_x$ | $-\frac{1}{2}+\Delta_y$ | 0 | $\Delta_x = -0.0020$; $\Delta_y = 0.0060$ |
| 4×O(4) | $-\frac{1}{2}+\Delta_x$ | $\Delta_y$ | $-\frac{1}{2}+\Delta_z$ | $\Delta_x = 0.0003, \Delta_y = 0.0001, \Delta_z = 0.0003$ |
| 1×O(5) | $-\frac{1}{2}+\Delta_x$ | $-\frac{1}{2}+\Delta_x$ | 0 | $\Delta_x \sim 0$ |

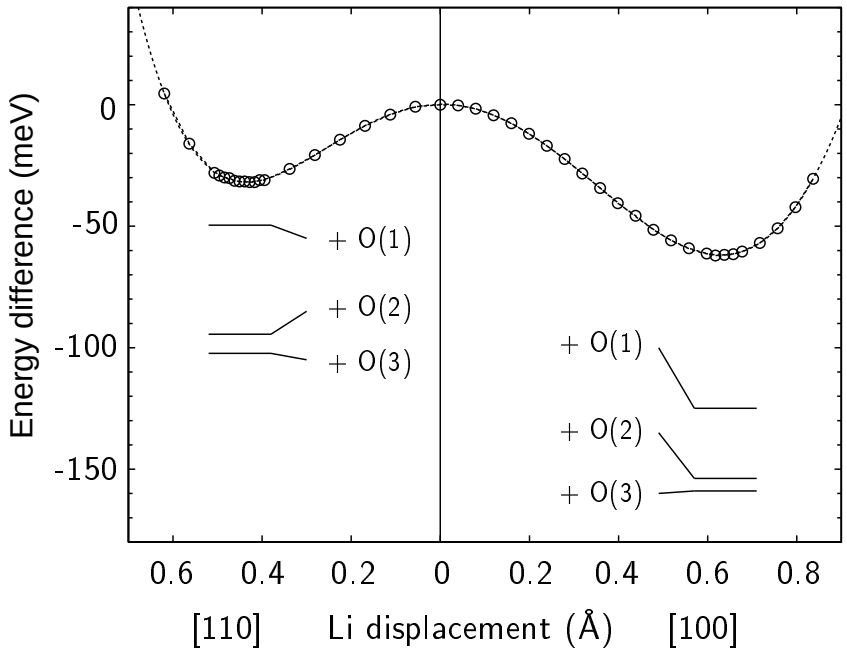


**FIGURE 2.** Total energy gain as function of [100] and [110] Li displacements without lattice relaxation (dashed line with open circles), and the total energy values after including the relaxation of three groups of nearest oxygen atoms.

The displaced Li ion with its neighboring oxygen atoms is shown schematically in Fig. 1 for the cases of [100] and [110] off-center displacements. The [100] displacement is known to occur in reality [8] whereas the [110] displacement represents a saddle point between two such adjacent and equivalent displaced configurations. Oxygen atoms are numbered according to their separation into several inequivalent groups.

The energy gain due to the Li off-center displacement is not directly measurable in an experiment, but there are estimations for the $90^0$-energy barrier via the saddle point between [100] and [010]-displaced positions to be 86 meV [10]. Our estimate of the energy difference between [100] and [110] minima is $\sim$30.2 meV, roughly two times larger than in the FP-LMTO calculation [13], but much less than the experimental estimate. The origin of this discrepancy, as has been mentioned in Ref. [13], is most probably related to the lattice relaxation around the displaced Li ion, that makes the net energy gain from the displacement larger, and the $90^0$-activation energy (involving now the displacement of many atoms) correspondingly higher. Indeed, the second harmonic generation-based estimates of the activation barrier [19] reveal two types of processes, apparently one involving the lattice relaxation (with the barrier height 86.2 meV) and another one that is too fast for the lattice to follow, with the barrier 14.7 meV.

In order to clarify this point, we performed a lattice relaxation of several shells of neighbors to the displaced Li ion, for the cases of [100] and [110] displacements.

The relaxed coordinates of atoms are given in Table 2, where the oxygen atoms are numbered consistently with Fig. 1. The total energy values resulting from the gradual inclusion of neighbor relaxation are shown in Fig. 2. We found the relaxation of twelve nearest oxygen atoms essential, and the effect of relaxing nearest Ta and more distant atoms to be negligible, in what regards the effect on the total energy. The energy gain in the fully relaxed [100]-displaced configuration, with respect to a non-relaxed central Li position, is 158.9 meV; the energy gain in the relaxed [110]-configuration is 102.3 meV. Therefore, the enhancement of the excitation barrier due to relaxation effects is by a factor of two, but still not sufficient to reach experimentally expected ∼86 meV. This discrepancy may be due to the fact that in reality the $90^0$-reorientation process of the impurity does not necessarily occur via the fully relaxed saddle-point configuration. Depending on the actual degree of relaxation around the saddle-point Li position, the barrier height is expected from Fig. 2 to be between ∼57 meV (full relaxation at the saddle point) to ∼127 meV (no relaxation).

## INTERACTING Li IMPURITIES IN $KTaO_3$

The experimental investigations of the diluted $K_{1-x}Li_xTaO_3$ system are numerous and include e.g. the nuclear magnetic resonance studies of relaxational dynamics associated with dipole reorientations [20], ultrasound attenuation measurements [21] and the measurements of the low-frequency shear modulus [22]. Due to different technical limitations, none of these methods allows to attain the ground state of system in the concentration range $x \leq 7\%$.

Up to now, there are reported only few theoretical studies of interacting Li impurities in $KTaO_3$, using mainly analytical approaches [23] or oversimplified shell model calculations [24], but there are no *ab initio* studies reported to our knowledge at this field. In order to get some theoretical predictions, check results of shell model calculations [24], and answer the question about the nature of the low-temperature phase of $K_{1-x}Li_xTaO_3$ at small concentrations of Li spin glasses or ferroelectrics, INDO calculations of Li-Li interaction in $KTaO_3$ may be of certain interest.

In the preliminary calculations done by now, we concentrated on two following subjects. First, we wanted to know how the interaction between Li impurities which substitute two neighboring K sites affects the energy characteristics and the lattice relaxation associated with each impurity. For this purpose, we allowed the simultaneous adjustment of the structure coordinates as listed in Table 3 (affecting both impurities and 20 oxygen neighbors). The labelling of atoms in Tab. 3 and the qualitative scheme of the relaxation pattern is shown in Fig. 3. The relaxation of Ta and K atoms was found to be much smaller than that of O neighbors. The energy gain that was 62 meV due to the [100] displacement of a single Li impurity and 159 meV for the oxygen relaxation taken into account, makes correspondingly 176 meV and 407 meV per two Li impurities. It indicates that a substantial Li-Li

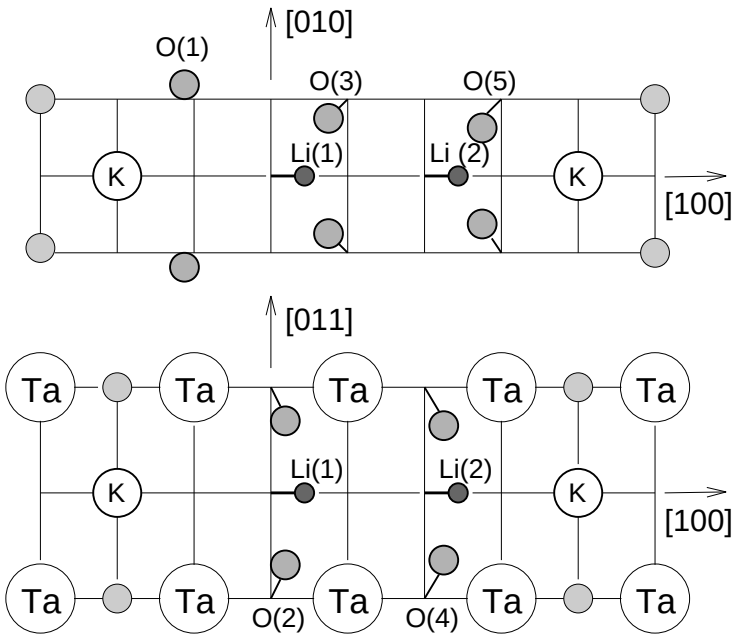


**FIGURE 3.** Off-center displacements of two nearest Li atoms and the relaxation pattern of 20 neighboring oxygen atoms.

interaction of the magnitude $E(2\text{Li}) - 2 \times E(\text{Li}) = 52$ meV for bare Li and 89 meV for Li with oxygen "cloud" indeed occurs and is enhanced by lattice polarization.

Second important characteristic is the strength and spatial distribution of the dipole field created by each Li impurity. In order to study it, we used the "probe" Li impurity at different lattice positions and displaced in different directions with respect to the "central" one. The "central" impurity was displaced along [100] by 0.62 Å, i.e. the equilibrium displacement for the single off-center Li ion. The "probe" impurity was allowed to relax along the given direction, and the interaction energy was extracted as a measure of the dipole field in crystal. The tested positions of the "probe" impurities in crystal are indicated in Fig. 4, and the resulting interaction energies – in Table 4. One can clearly see the anisotropy of the

**TABLE 3.** Lattice relaxation around two nearest Li impurities

| Atom | Lattice coordinates | | | Displacement |
|---|---|---|---|---|
| Li(1) | $\Delta_x$ | 0 | 0 | $\Delta_x = 0.1550$ |
| Li(2) | $1+\Delta_x$ | 0 | 0 | $\Delta_x = 0.178$ |
| O(1) | $-\frac{1}{2}+\Delta_x$ | $\pm(\frac{1}{2}+\Delta_{yz})$ | 0 | $\Delta_x = -0.0022$; $\Delta_{yz} = 0.0022$ |
| O(2) | $\Delta_x$ | $\pm(\frac{1}{2}+\Delta_{yz})$ | $\pm(\frac{1}{2}+\Delta_{yz})$ | $\Delta_x = 0.0075$; $\Delta_{yz} = -0.0028$ |
| O(3) | $\frac{1}{2}+\Delta_x$ | $\pm(\frac{1}{2}+\Delta_{yz})$ | 0 | $\Delta_x = -0.0074$; $\Delta_{yz} = -0.0082$ |
| O(4) | $1+\Delta_x$ | $\pm(\frac{1}{2}+\Delta_{yz})$ | $\pm(\frac{1}{2}+\Delta_{yz})$ | $\Delta_x = 0.0080$; $\Delta_{yz} = -0.0032$ |
| O(5) | $\frac{3}{2}+\Delta_x$ | $\pm(\frac{1}{2}+\Delta_{yz})$ | 0 | $\Delta_x = -0.0057$; $\Delta_{yz} = -0.0125$ |

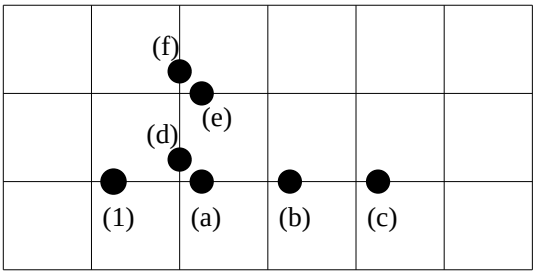


**FIGURE 4.** Distribution of interacting Li impurities in 3×3×6 extended $KTaO_3$ supercell. There are considered interaction between Li(1) and another Li placed consequently in a,b,c,d,e,f positions.

**TABLE 4.** Effective interaction energy $E_{int.}$ and equilibrium displacement $\Delta$ of the second Li atom (a–f) for different mutual configurations displacements. The displacement of Li(1) is fixed at 0.62 Å along [100].

| Li pair | $E_{int}$ (meV) | $\Delta$ (Å) | Li pair | $E_{int}$ (meV) | $\Delta$ (Å) |
|---|---|---|---|---|---|
| 1–a | 61.6 | 0.72 | 1–d | 28.52 | 0.677 |
| 1–b | 10.29 | 0.633 | 1–e | 5.93 | 0.633 |
| 1–c | 7.56 | 0.629 | 1–f | 17.91 | 0.657 |

interaction field. The numerical values may be somehow affected by the choice of even larger supercell in subsequent calculations. It is noteworthy, however, that the interaction strength decreases with the distance faster than it was found in the shell model calculations [24].

## SUMMARY

In the present study of two different point defects in perovskites by means of a semiempirical INDO method, based on the comparison with *ab initio* calculation results, we established the following. The ground state of the $F$ center in $KNbO_3$ is associated with a strong symmetrical relaxation of two nearest Nb atoms outwards relative to the O vacancy. We presented a strong argument that the 2.7 eV absorption band observed in electron-irradiated crystals could be due to the $F$-type centers, and predicted the existence of two additional absorption bands (at 3.04 eV and 3.10 eV) for the same defect in the orthorhombic phase of $KNbO_3$. In the analysis of single and interacting off-center Li impurities in $KTaO_3$ we estimated the lattice relaxation around impurities and the characteristic interaction energies, depending on the distance between the defects and their mutual orientation. The interaction energies are lower and less long-ranged than it was estimated from earlier shell-model calculation.

**Acknowledgments**

Financial support of the Deutsche Forschungsgemeinschaft (SFB 225, Graduate College) is greatly acknowledged.

# REFERENCES

1. P. Günter and J.-P. Huignard (eds.) *Photorefractive Materials and Their Application* (Topics in Applied Physics, **61, 62**), Berlin, Heidelberg: Springer-Verlag, 1988.
2. L. Shiv, J. L. Sørensen, E. S. Polzik, and G. Mizell, *Optics Letters* **20**, 2271 (1995).
3. J. H. Crawford, Jr., *Nucl. Inst. Meth. B* **1** 159 (1984); J. -M. Spaeth, J. R. Niklas, and R. H. Bartram, *Structural Analysis of Point Defects in Solids* (Springer series in Solid State Sciences, vol. 43), Berlin, Heidelberg: Springer-Verlag, 1993.
4. E. R. Hodgson, C. Zaldo, and F. Agullo-López, *Solid State Commun.* **75**, 351 (1990).
5. E. A. Kotomin, R. I. Eglitis, and A. I. Popov, *J. Phys.: Condens. Matter* **9**, L315 (1997).
6. S. A. Prosandeyev, A. V. Fisenko, A. I. Riabchinski, A. I. Osipenko, I. P. Raevski, and N. Safontseva, *J. Phys.: Condens. Matter*,**8**, 6705 (1996).
7. R. I. Eglitis, N. E. Christensen, E. A. Kotomin, A. V. Postnikov, and G. Borstel, *Phys. Rev. B* **56**, 8599 (1997).
8. Y. Yacoby and S. Just, *Solid State Commun.* **15**, 715 (1974).
9. F. Borsa, U. Höchli, J. J. van der Klink, and D. Rytz, *Phys. Rev. Lett.* **45**, 1884 (1980); U. T. Höchli, K. Knorr, and A. Loidl, *Adv. Phys.* **39**, 405 (1990).
10. J. J. van der Klink and S. N. Khanna, *Phys. Rev. B* **29**, 2415 (1984).
11. M. G. Stachiotti and R. L. Migoni, *J. Phys.: Condens. Matter.* **2**, 4341 (1990).
12. M. Exner, C. R. A. Catlow, H. Donnerberg, and O. F. Schirmer, *J. Phys.: Condens. Matter* **6**, 3379 (1994).
13. A. V. Postnikov, T. Neumann, and G. Borstel, *Ferroelectrics*, **164**, 101 (1995).
14. R. E. Eglitis, A. V. Postnikov, and G. Borstel, *Phys. Rev. B* **55**, 12976 (1997).
15. A. Shluger, *Theoret. Chim. Acta* (Berl.) **66**, 355 (1985); E. Stefanovich, E. Shidlovskaya, A. Shluger, and M. Zakharov, *Phys. Status Solidi B* **160**, 529 (1990); A. Shluger and E. Stefanovich, *Phys. Rev. B* **42**, 9664 (1990).
16. R. I. Eglitis, A. V. Postnikov, and G. Borstel, *Phys. Rev. B* **54**, 2421 (1996).
17. M. Methfessel, *Phys. Rev. B* **38**, 1537 (1988); M. Methfessel, C. O. Rodriguez, and O. K. Andersen, *ibid.* **40**, 2009 (1989).
18. R. A. Evarestov and L. A. Lovchikov, *Phys. Status Solidi B* **93**, 469 (1977).
19. P. Voigt and S. Kapphan, *J. Phys. Chem. Solids* **55**, 853 (1994).
20. J. J. van der Klink and F.Borsa, *Phys. Rev. B* **30**, 52 (1992); S. Rod, F. Borsa, and J. J. van der Klink, *ibid.* **38**, 2267 (1988).
21. P. Doussineau, C. Frenois, A. Lavelut, and S. Ziolkievicz, *J. Phys.: Condens. Matter* **3**, 8369 (1991).
22. U. Höchli, J. Hessinger, and K. Knorr, *J. Phys.: Condens. Matter* **3**, 8377 (1991).
23. B. E. Vugmeister and M. D. Glinchuk, *Rev. Mod. Phys.* **82**, 993 (1990).
24. M. G. Stachiotti, R. L. Migoni, H. M. Christen, J. Kohanoff, and U. Höchli, *J. Phys.: Condens. Matter* **6**, 4297 (1994).